Hindawi Publishing Corporation
International Journal of Photoenergy
Volume 2014, Article ID 414281, 9 pages
http://dx.doi.org/10.1155/2014/414281

Research Article

A Facile and Waste-Free Strategy to Fabricate Pt-C/TiO_2 Microspheres: Enhanced Photocatalytic Performance for Hydrogen Evolution

Hui Li,[1] Xiaoyan Zhang,[2] and Xiaoli Cui[1]

[1] *Department of Materials Science, Fudan University, Shanghai 200433, China*
[2] *Key Laboratory of Materials for High-Power Laser, Shanghai Institute of Optics and Fine Mechanics, Chinese Academy of Sciences, Shanghai 201800, China*

Correspondence should be addressed to Xiaoli Cui; xiaolicui@fudan.edu.cn

Received 14 June 2014; Revised 11 July 2014; Accepted 12 July 2014; Published 5 August 2014

Academic Editor: Tian-Yi Ma

A facile and waste-free flame thermal synthesis method was developed for preparing Pt modified C/TiO_2 microspheres (Pt-C/TiO_2). The photocatalysts were characterized with X-ray diffraction, field emission scanning electron microscopy, transmission electron microscope, ultraviolet-visible (UV-vis) diffuse reflectance spectra, X-ray photoelectron spectroscopy, and thermogravimetry analysis. The photocatalytic activity was evaluated by hydrogen evolution from water splitting under UV-vis light illumination. Benefitting from the electron-hole separation behavior and reduced overpotential of H+/H_2, remarkably enhanced hydrogen production was demonstrated and the photocatalytic hydrogen generation from 0.4 wt% Pt-C/TiO_2 increased by 22 times. This study also demonstrates that the novel and facile method is highly attractive, due to its easy operation, requiring no post treatment and energy-saving features.

1. Introduction

Photocatalytic water splitting for hydrogen evolution has attained great significance since hydrogen has been considered to be one of the ideal green fuels and can be used directly in fuel cells as well as in fuel cell-powered vehicles. In recent years, water splitting to produce hydrogen based on semiconductors has attracted tremendous attention [1–6]. As a typical semiconductor material, TiO_2 has been widely studied in photocatalytic area due to its abundance, photostability, chemical inertness, and low toxicity [7–10]. However, the high recombination rate of photogenerated electrons and holes in TiO_2 would limit its photocatalytic activity [11, 12]. The relatively low light harvesting efficiency behaves as another drawback of TiO_2 in its photocatalytic utilization [13, 14]. These factors strongly inhibit the extensive use of naked TiO_2 in solar-driven water splitting.

In the past decades, many attempts have been made to explore new avenues to prolong the life time of photogenerated carriers for higher quantum efficiency or to narrow the band gap of TiO_2 for a much larger visible fraction in its light absorption spectrum, such as modification of TiO_2 through implantation of metal ions [15, 16], doping of nonmetal atoms [17, 18], and combination with other components, including secondary semiconductors [19, 20], noble metals [21, 22], and dyes [23, 24].

It was once proposed that carbon species incorporated in TiO_2 can act as sensitizers [25, 26], thus enhancing the photocatalytic activity of TiO_2 by expanding light absorption range into visible region. There comes introduction of several nanostructured carbon materials such as carbon nanotubes [27] and graphene [28] for enhancement of photocatalytic H_2 production. Besides, Pt nanoparticles are excellent candidates to serve as cocatalysts since their Fermi-energy levels are normally more positive than the conduction band of TiO_2. Thus it can attract the photon-excited electrons to suppress the possible electron-hole recombination [29, 30].

Great efforts have been made to synthesize Pt modified TiO_2 composites with high electrochemical or photocatalytic activity [31–36]. Ran et al. [2] recently addressed the fact that

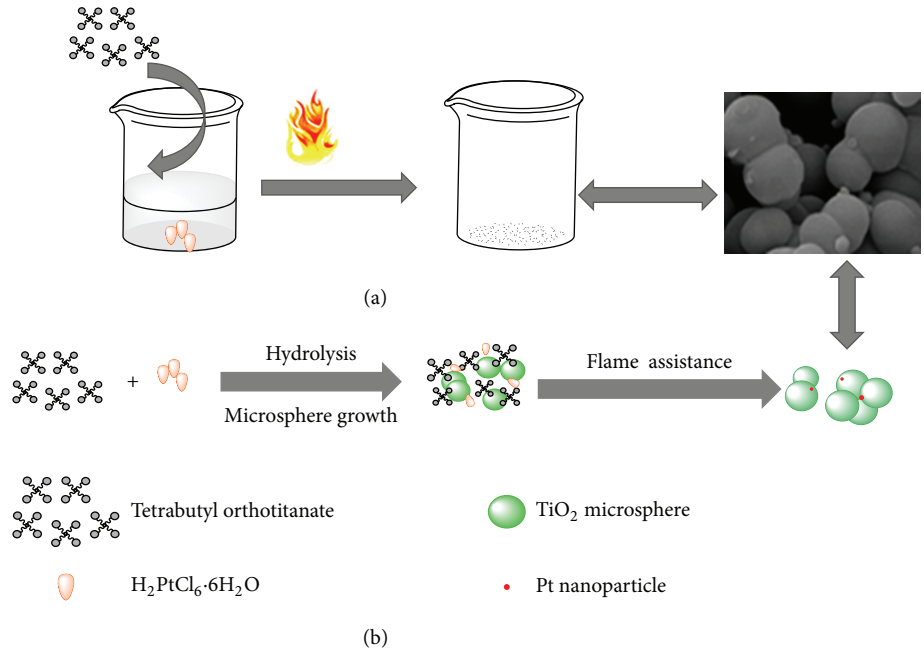

Scheme 1: (a) Schematic illustration of the fabrication procedure of Pt-C/TiO_2 composite. (b) Schematic representation of Pt-C/TiO_2 microsphere growth process.

cocatalysts especially Pt metals are a key factor in achieving higher photocatalytic activity in most semiconductor-based photocatalytic systems. Sreethawong et al. [34] prepared N-doped nanocrystalline mesoporous-assembled TiO_2; various Pt contents were loaded onto the nanocomposites through the incipient wetness impregnation method. It was observed that the impregnation of Pt considerably improved its photocatalytic H_2 production activity and the optimum Pt loading content was 1.3 wt%. Ismail and coworkers [35] synthesized Pt/RuO_2-TiO_2 photocatalysts by using photoreduction method and followed by calcination at 450°C for 4 h. The as-prepared samples exhibited excellent photocatalytic activity for photooxidation of CH_3OH under UV light irradiation. Wang's group [36] obtained Pt decorated $TiO_{2-x}N_x$ *via* a one-pot route. Enhanced photocatalytic activity for degradation of propylene under visible light was achieved. The improved performance was ascribed to the synergistic effect of oxygen vacancies and dopants of N and Pt. Although these methods have their own advantages, they are more or less limited by high temperatures or special facilities. Therefore, developing a more facile approach to fabricate Pt based TiO_2 photocatalysts is still very necessary.

Recently, we have reported an easy route for constructing C/TiO_2 [37], Fe-C/TiO_2 [16], SiO_x-C/TiO_2 [38], and Ta_2O_5 [3] photocatalysts. Our strategy featured with short reaction time, easy operation, low cost, waste free and only one step to obtain the final TiO_2. In the present work, we further introduced Pt to modify C/TiO_2 in order to achieve higher activity for the photocatalysts. The synthesis of Pt-C/TiO_2 nanomaterials via the simple flame thermal approach was achieved and their higher performance was revealed as desired. The influence of Pt content on the phase, microstructures, and optical and photocatalytic properties was investigated in detail.

2. Experimental

2.1. Materials. Tetrabutyl orthotitanate (TBOT, CP) was purchased from Sinopharm Group Chemical Reagent Company, and the stated purity was 98%; absolute ethanol (>97%) and chloroplatinic acid ($H_2PtCl_6{\cdot}6H_2O$, AR) were obtained from Shanghai Zhenxing No. 1 Chemical Plant. All of the chemicals were used as received.

2.2. Preparation of Pt-C/TiO_2. A series of Pt-C/TiO_2 nanocomposites were fabricated by using the aforementioned chemicals as starting materials, as illustrated in Scheme 1. Briefly, the specified weight of $H_2PtCl_6{\cdot}6H_2O$ was added into a standard beaker (150 mL) containing 35 mL of ethanol and 5 mL of TBOT by stirring. The obtained stable solutions were ignited by a match stick under ordinary conditions. Gray powders were obtained after gentle burning for about 30 min. The final samples with different amount of Pt: C/TiO_2 mass ratios were labeled as 0.1 wt%, 0.4 wt%, and 0.6 wt% Pt-C/TiO_2, respectively. For comparison, C/TiO_2 powders were also prepared by a similar procedure except for the absence of Pt precursor [37].

2.3. Characterizations. The structure and phase composition of the samples were examined by X-ray diffraction (XRD) on a Bruker D/8 advanced diffractometer using Cu Kα radiation. The morphologies were characterized by field emission scanning electron microscope (FE-SEM: Philips XL30) and transmission electron microscope (TEM: JEOL

Table 1: Crystal sizes, absorption edges, and band gap energies of the synthesized samples.

Sample	P25	C/TiO_2	0.1 wt% Pt-C/TiO_2	0.4 wt% Pt-C/TiO_2	0.6 wt% Pt-C/TiO_2
D_{TiO_2} (nm)[a]	20.9	19.6	20.2	20.6	20.1
Absorption edge (nm)	394	423	438	456	471
Band gap (eV)	3.15	2.93	2.83	2.72	2.63

[a]D_{TiO_2} is calculated from the most intense diffraction peak (101) of XRD spectra of the samples.

JEM-2011, Japan). A Cary-50 Scan UV-Vis spectrophotometer was used to measure the UV-vis diffuse reflectance spectra (DRS) with the scan range in the region of 200–800 nm. The instrument employed for X-ray photoelectron spectroscopy (XPS) studies was a RBD upgraded PHI-5000 C ESCA system (Perkin Elmer) with Al/Mg Kα radiation. The binding energy was corrected using the C1s level at 284.6 eV as an internal standard. Thermogravimetry analysis (TGA) was carried out on a SDT-Q600 (TA Company, USA) instrument with a heating rate of 10°C min^{-1} using oxygen as the purge gas.

2.4. Photocatalytic Activity Measurements. The photocatalytic activity of samples was measured under UV-vis light illumination by using 500 W Xe lamp (CHF-XM35, Trusttech Co., Ltd., Beijing) as light source. The light intensity was kept at 180 mW cm^{-2}, which was measured by an optical power meter (1 L 1400 A, International Light). The experiments were carried out in a closed quartz reactor system. Typically, the photocatalysts (65 mg) were suspended in an aqueous methanol solution (80 mL of distilled water, 20 mL of methanol) by means of a magnetic stirrer within the reactor. Prior to the experiment, the mixture was dispersed by ultrasound treatment for 15 min, followed by purging N_2 gas for 30 min. The amount of evolved H_2 was determined by a GC7900 gas chromatograph (thermal conductivity detector, molecular sieve 5 A, 99.999% N_2 carrier).

3. Results and Discussion

3.1. XRD Patterns. Figure 1 shows the XRD patterns of the synthesized Pt-C/TiO_2 powders, and the patterns can be well indexed to the anatase TiO_2, which were determined directly without any subsequent high temperature calcination. The peaks corresponding to Pt could not be detected in Figures 1(c)–1(e); this is mainly ascribed to the relatively low content of this element in the nanocomposites. Similar results can also be found in the previous report [31]. The average crystallite sizes (D) calculated from the main diffraction peaks using Scherrer equation are present in Table 1. It can be seen that there is nearly no difference in the D value among all the samples (*ca.* 20 nm), implying that the introduction of Pt did not alter the crystallite size of TiO_2.

3.2. SEM and TEM Images. The morphologies of the samples with various Pt content were characterized by SEM. As shown in Figure 2, the microsphere with a diameter of ~0.5 to 2.0 μm was observed for all of the prepared samples. It has been recognized that the microspheres can allow multiple reflections and scattering of incident light, which enhances

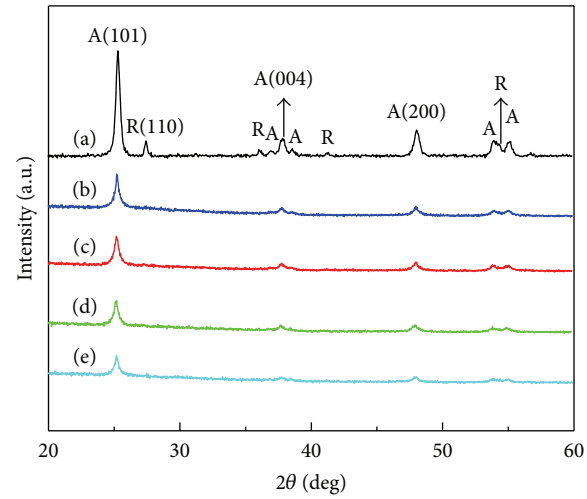

Figure 1: XRD patterns of P25 (a), C/TiO_2 (b), and Pt-C/TiO_2 composites (c)–(e). The content of Pt is 0.1 wt% (c), 0.4 wt% (d), and 0.6 wt% (e), respectively. (A: anatase, R: rutile.)

light harvesting and increases the quantity of photogenerated electrons and holes [37]. Therefore, it is anticipated that the photocatalytic performance will be improved for the samples. As compared with C/TiO_2, the introduction of Pt does not cause noticeable change in morphology, but more microspheres are fused together with increasing Pt content, and this change is observed more clearly in Figure 2(d). These demonstrations reveal that limited fraction of Pt is required to obtain relatively dispersed microspheres.

Figure 3 depicts the TEM images of 0.4 wt% Pt-C/TiO_2 nanocomposite. As displayed in Figure 3(a), TiO_2 microsphere is composed of small primary nanoparticles of about 20 nm in diameter; this observation is in agreement with the XRD evaluation. The HRTEM image is presented in Figure 3(b); one can clearly observe that the lattice fringes are characteristics of the anatase TiO_2 crystal, in which the d-spacing of 0.35 nm corresponds to the distance between the (101) planes [39]. The corresponding selected-area electron diffraction (SAED) pattern of the nanocomposite (Figure 3(b), inset) further provides evidence of anatase structure of TiO_2 with polycrystalline feature. This finding is consistent with the XRD results. Subsequent chemical composition analysis of this material by EDX spectroscopy shows the presence of Pt, C, Ti, and O elements in the nanocomposite (Figure 3(c)), confirming that the obtained nanocomposite consists of Pt. In order to investigate the shape and size of Pt particles, we synthesized an additional

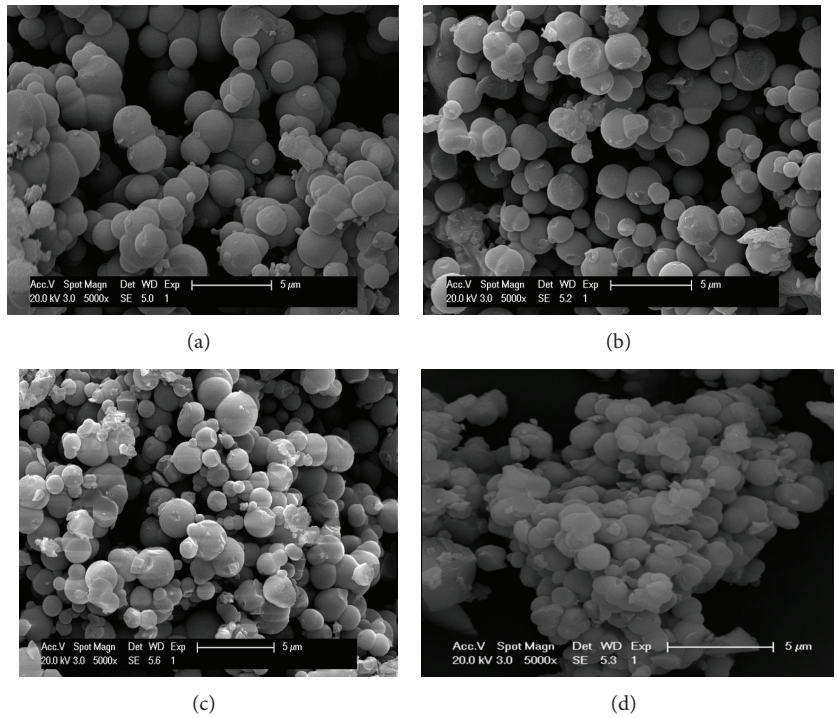

Figure 2: SEM images of the samples of C/TiO_2 (a), 0.1 wt% Pt-C/TiO_2 (b), 0.4 wt% Pt-C/TiO_2 (c), and 0.6 wt% Pt-C/TiO_2 (d), respectively.

sample with Pt fraction up to 1.2 wt%. TEM image of the sample is shown in Figure 3(d). Interestingly, many spherical shaped particles with diameter of 2 to 5 nm can be easily found; the lattice fringes of 0.23 nm match the crystallographic planes of Pt (111) [31]. This result further revealed the presence of Pt nanoparticles in the resulted samples.

3.3. Formation Mechanism of TiO_2 Spheres. Scheme 1 shows possible formation mechanism of TiO_2 microspheres. Self-generated water from ethanol combustion promoted the hydrolysis of TBOT molecules to form TiO_2 nanoparticles. Then nucleation and growth of the particles by coagulation and condensation occurred along the axial direction of the flame. After this period, the nanoparticles are surrounded by the solution, where the water content, gradually increasing in the system, leads to the continuous hydrolysis of TBOT. Nucleated clusters of TiO_2 particles quickly aggregated to form solid spheres and crystalized to anatase phase at the elevated temperature [40]. Due to the rapid hydrolysis of TBOT and abrupt shrinkage of the droplets, during the firing in air, the final TiO_2 powders consist of a large amount of aggregated spheres [41].

When small amount of $H_2PtCl_6{\cdot}6H_2O$ is present in the solution, thermal decomposition of $H_2PtCl_6{\cdot}6H_2O$ would occur under the pyrolysis condition and Pt particles are simultaneously formed. Since the fast thermolysis and low fraction of $H_2PtCl_6{\cdot}6H_2O$, the transformation to Pt reached so fast that the pyrolysis rate can continually exceed the hydrolysis and condensation rate of TBOT. Consequently, it is assumed that Pt nanoparticles may be embedded in the C/TiO_2 nanocomposite.

3.4. UV-Vis Diffuse Reflectance Spectra. Figure 4 displays the UV-vis diffuse reflectance spectra of the as-prepared samples. A strong absorption in the visible light region is observed for the Pt-C/TiO_2 photocatalysts. The results also indicate that $PtCl_6^{2-}$ complexes transformed to Pt completely since there is no absorption band from $PtCl_6^{2-}$ complexes, which would exhibit a ligand-to-metal charge transfer band with a maximum at 262 nm and two bands at around 360 and 480 nm corresponding to d-d transitions [42, 43]. Furthermore, the absorption edges increased linearly with the increase of Pt concentration (see Table 1). The value of optical band gap energy of 3.15 eV was calculated for pure TiO_2 according to the equation of E_g (eV) = $1240/\lambda_g$ [44], which is the same as theoretical value of the anatase phase. Narrowed band gap energies were obtained for the as-synthesized Pt-C/TiO_2 composites, and the data are presented in Table 1. The stronger absorption intensity and longer absorption edge can be attributed to the following factors: (i) carbon in samples can act as sensitizer, which will expand light absorption range into visible region [45]; (ii) Pt-C/TiO_2 photocatalysts probably exhibit surface plasmon resonance (SPR) due to the presence of Pt particles [46], which will extend the absorption edge to visible light. The SPR peak for the Pt nanoparticles is typically below 450 nm with broad peak shape; thus usually it can hardly be observed [47, 48].

3.5. XPS Analysis. To investigate the chemical state of elements in the sample, XPS analysis is conducted and the results are presented in Figure 5. Figure 5(a) is the XPS spectra of a survey spectrum for a typical sample. Elements of Ti, O, C, and Pt can be detected in this spectrum. In the Ti 2p spectrum

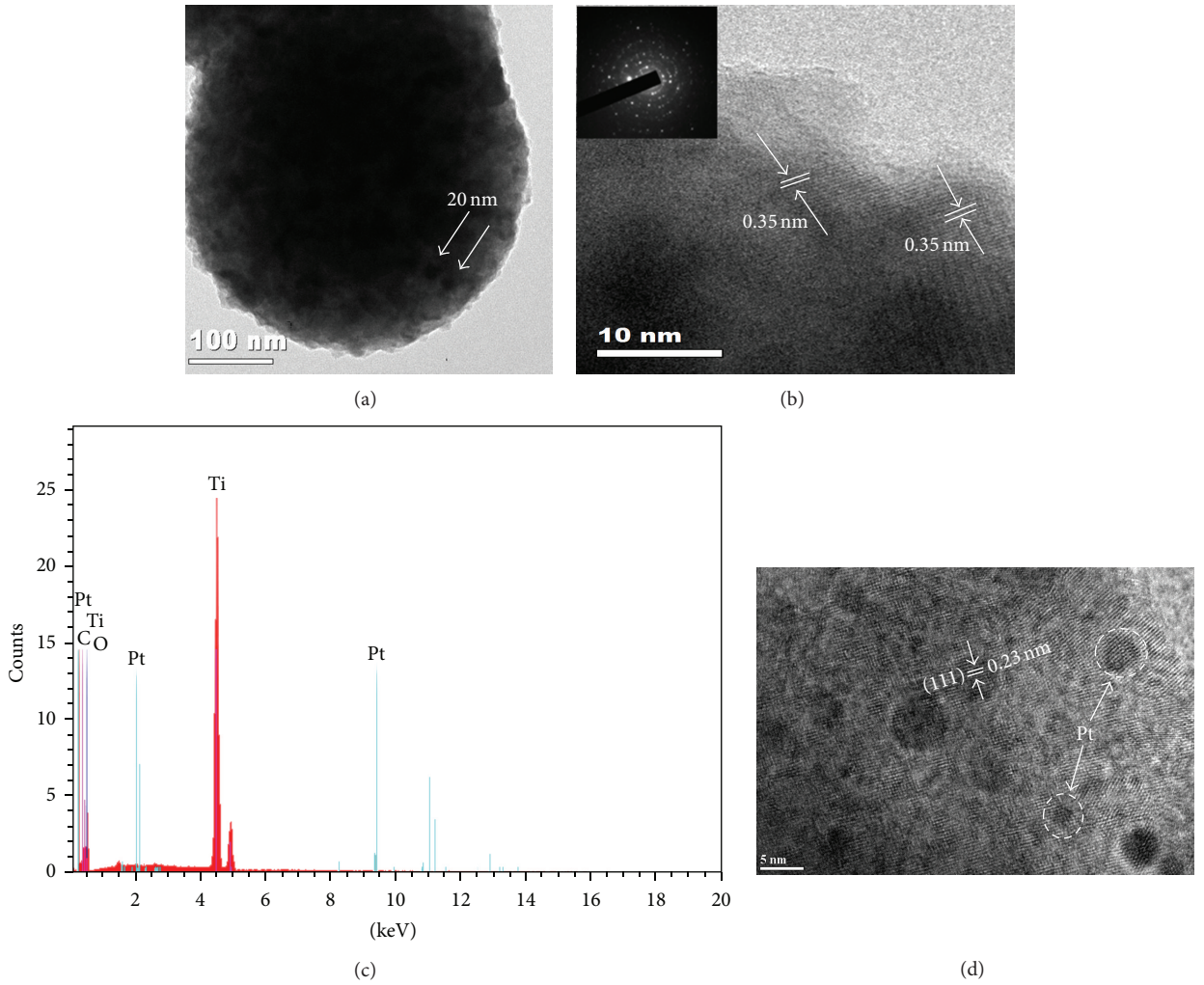

Figure 3: (a) Representative TEM and HRTEM images of the material: (a) TEM image of 0.4 wt% Pt-C/TiO_2; (b) HRTEM image of 0.4 wt% Pt-C/TiO_2; inset is the SAED pattern; (c) EDX spectrum of the composite; (d) HRTEM image of 1.2 wt%Pt-C/TiO_2.

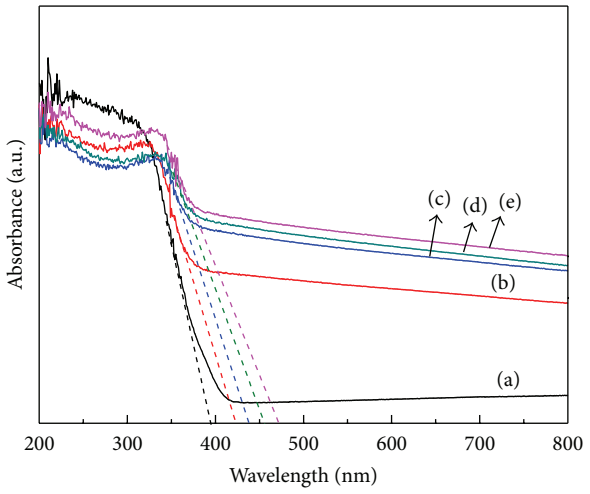

Figure 4: UV-vis diffuse reflectance spectra of P25 (a), C/TiO_2 (b), and Pt-C/TiO_2 composites (c)–(e). The content of Pt is 0.1 wt% (c), 0.4 wt% (d), and 0.6 wt% (e), respectively.

of TiO_2 (Figure 5(b)), there are two peaks centered at 458.5 eV and 464.2 eV, which are characteristic of the Ti 2p3/2 and Ti 2p1/2 for Ti (IV) [49, 50], respectively. Figure 5(c) shows the XPS spectrum of C 1s of the sample. The peak at 284.6 eV is ascribed to elemental carbon, arising from the incomplete burning of organic compounds [38]. The other small peak at higher binding energies of 288.5 eV is attributed to C–O bonds [51], which originates from the insufficient hydrolysis of TBOT. It is to be noted that the absence of the characteristic binding energy of 281.0 eV for C–Ti bonds indicates that the carbon did not exist as a dopant; that is, most of the carbon species in TiO_2 are present as elemental state [52]. Figure 5(d) displays XPS spectrum for Pt 4f. Two peaks at around 71.4 eV and 74.7 eV are assigned to 4f7/2 and 4f5/2 of Pt (0), respectively [53]. This result confirmed the presence of metallic Pt in the nanocomposite, which is in line with the observations from TEM and UV-vis DRS.

3.6. TGA Curve. The thermal behavior of a typical sample is probed by measuring thermal analysis and TGA curve is

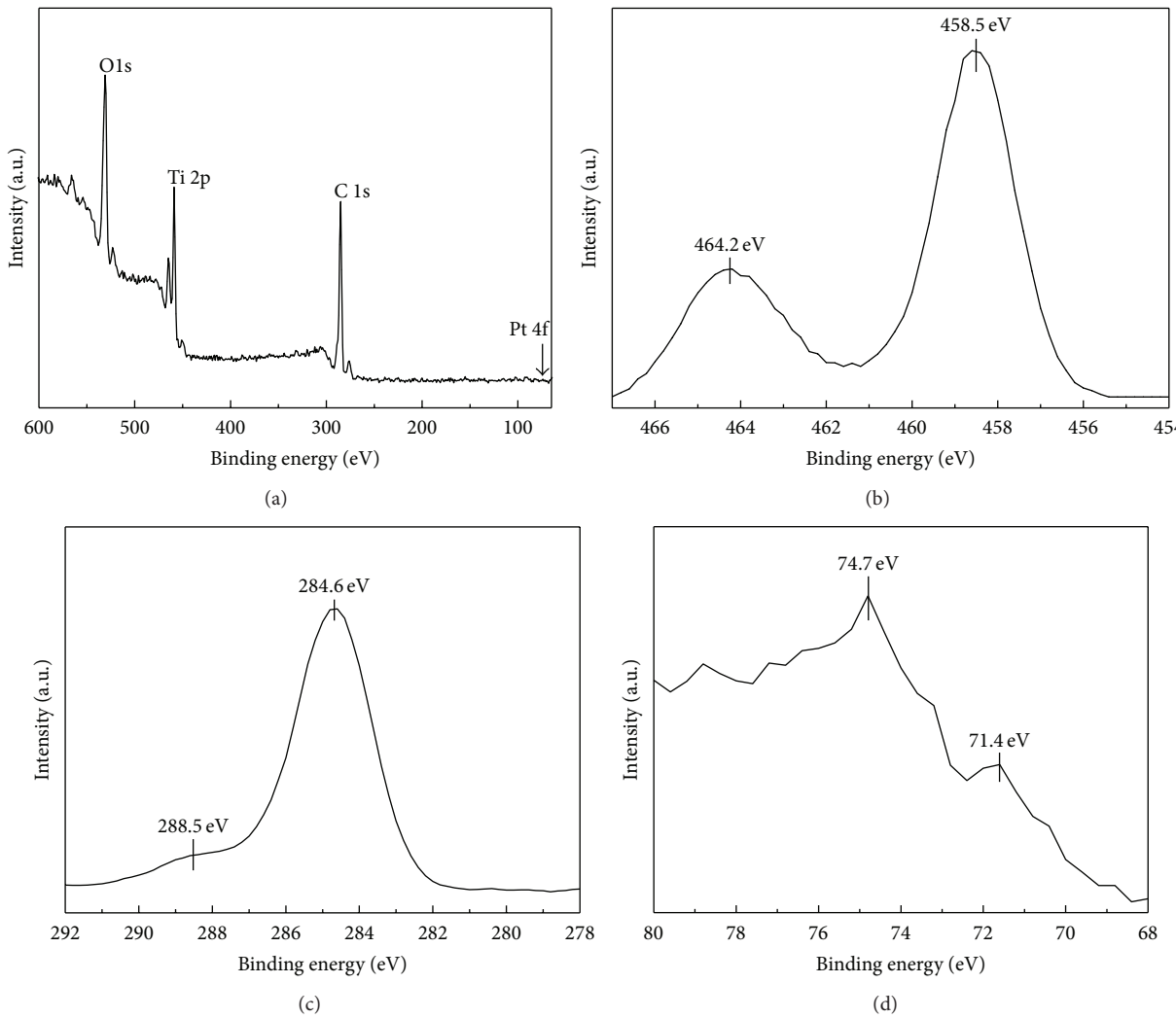

Figure 5: XPS spectra of 0.4 wt% Pt-C/TiO_2 (a), Ti 2p (b), C1s (c), and Pt 4f (d).

presented in Figure 6. Three main weight losses can be seen at about 100°C, 300°C, and 600°C, respectively. The weight loss at 100°C originates from water and residual ethanol evaporation. The second step around 300°C is ascribed to the decomposition of residual organics on the surface of TiO_2. Another peak is attributed to the oxidation of carbon species. The peak relevant to Pt oxidation has not been found within 800°C, suggesting the high stability of Pt in the nanocomposite.

3.7. Photocatalytic H_2 Production Activity. Photocatalytic activities of the samples were assessed and compared with that of commercial P25 by determining the hydrogen production from aqueous methanol solution. Such a sacrificial agent system is widely used in the studies of photocatalytic H_2 production [34, 54, 55]. As depicted in Figure 7, the hydrogen evolution on P25 is negligible under the applied experimental conditions. It should be reasonable to detect hydrogen evolution from C/TiO_2. Since carbon in TiO_2 is likely to carry out a charge transfer process and is responsible for the photosensitization of TiO_2 [45, 56]. The generated hydrogen amount is significantly increased when taking the samples of Pt-C/TiO_2 as photocatalysts. The improved photocatalytic performance is mainly because the modified Pt is able to capture electrons and decrease the overpotential of H^+/H_2, thus leading to the decrease of the electron-hole pairs recombination [57]. The maximum H_2 evolution is achieved for about 5.1 μmol on the sample of 0.4 wt%Pt-C/TiO_2 after 3 h irradiation. Significantly, the value is about 22 times that of P25. Nevertheless, the amount of H_2 decreased to 4.8 μmol when Pt concentration gets to 0.6 wt%. This phenomenon agrees with that of previous reports [55, 58]. The reason probably is that excessive concentration of Pt nanoparticles will lead to abundant Pt-trapped electrons, which enable easier encounters between the diffusing holes and the Pt-trapped electrons. Consequently, Pt becomes more of electron-hole recombination centers instead of electron-hole separation enhancers [59].

It should be recognized that the activity for H_2 evolution is relatively low and more work is necessary to further increase the H_2 production. While in this work, the amount of Pt is relatively smaller to obtain the optimum photocatalytic

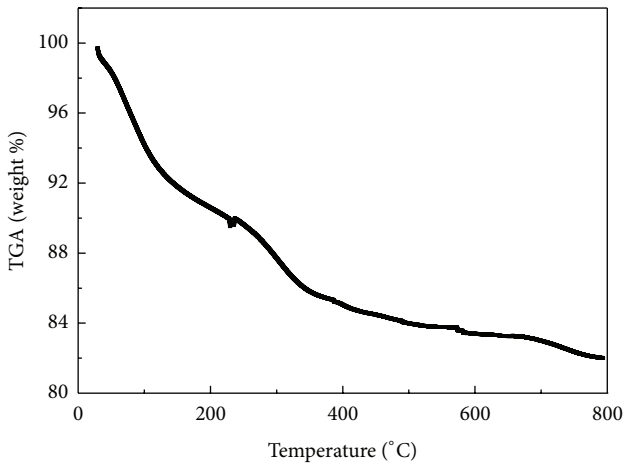

Figure 6: TGA curve of 0.4 wt% Pt-C/TiO_2 powders.

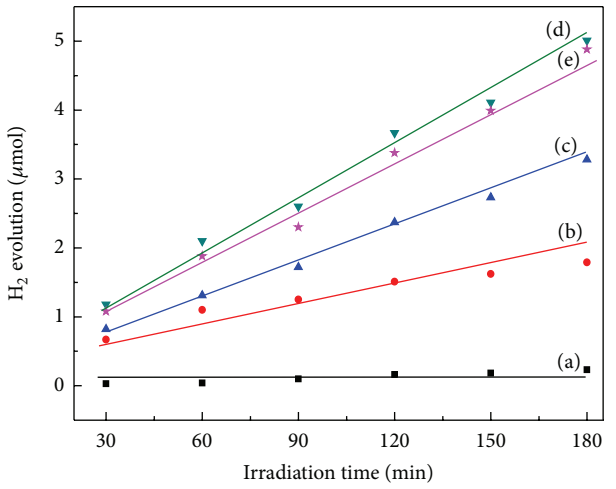

Figure 7: Time course of hydrogen evolution under UV-vis light irradiation. (a) P25, (b) C/TiO_2, (c) 0.1 wt% Pt-C/TiO_2, (d) 0.4 wt% Pt-C/TiO_2, and (e) 0.6 wt% Pt-C/TiO_2.

activity compared with that reported in literatures [34, 60]. The reduced Pt content on TiO_2 will be important both from a commercial and an ecological point of view. The photocatalytic efficiency of hydrogen evolution is expected to further improve through the better design of hydrogen evolution reactor, the modification of nanocomposites, and the optimization of energy levels of photocatalysts. Corresponding experiments are in progress in this laboratory and the results will be reported in due course.

4. Conclusions

In summary, we presented a novel and facile flame thermal method for the preparation of Pt modified C/TiO_2 microspheres in the first time and demonstrated their high photocatalytic performance for H_2 evolution. The as-prepared anatase TiO_2 powders show enhanced absorption behavior and obvious red shift in photoresponse towards visible light region. Compared to commercial P25, the resulted samples show significantly improved photocatalytic activity. Given the relatively simple, rapid, scalable, highly efficient, and energy-saving properties of this method, it is reasonable to conclude that this technique will be transferable to the fabrication of other modified TiO_2 microspheres.

Conflict of Interests

The authors declare that there is no conflict of interests regarding the publication of this paper.

Acknowledgments

This work was supported by the Natural Science Foundation of China (no. 21273047) and the National Basic Research Program of China (nos. 2012CB934300, 2011CB933300). The authors thank Ms. Ma Xiaoqing for editing the paper. We also appreciate the referee's very valuable comments, which have greatly improved the quality of the paper.

References

[1] A. Ishikawa, T. Takata, J. N. Kondo, M. Hara, H. Kobayashi, and K. Domen, "Oxysulfide Sm2Ti2S2O5 as a stable photocatalyst for water oxidation and reduction under visible light irradiation ($\lambda \leq 650$ nm)," *Journal of the American Chemical Society*, vol. 124, no. 45, pp. 13547–13553, 2002.

[2] J. R. Ran, J. Zhang, J. G. Yu, M. Jaroniecc, and S. Z. Qiao, *Chemical Society Reviews*, 2014.

[3] J. Li, X. Chen, M. Sun, and X. Cui, "A facile flame assisted approach to fabricate Ta_2O_5 microspheres," *Materials Letters*, vol. 110, pp. 245–248, 2013.

[4] Y. Wang, J. Yu, W. Xiao, and Q. Lia, "Microwave-assisted hydrothermal synthesis of graphene based Au–TiO_2 photocatalysts for efficient visible-light hydrogen production," *Journal of Materials Chemistry A*, vol. 2, no. 11, pp. 3847–3855, 2014.

[5] S. K. Parayil, H. S. Kibombo, C. Wu et al., "Synthesis-dependent oxidation state of platinum on TiO_2 and their influences on the solar simulated photocatalytic hydrogen production from water," *Journal of Physical Chemistry C*, vol. 117, no. 33, pp. 16850–16862, 2013.

[6] J. R. Ran, J. G. Yu, and M. Jaroniec, "$Ni(OH)_2$ modified CdS nanorods for highly efficient visible-light-driven photocatalytic H_2 generation," *Green Chemistry*, vol. 13, no. 10, pp. 2708–2713, 2011.

[7] X. Shao, W. Lu, R. Zhang, and F. Pan, "Enhanced photocatalytic activity of TiO_2-C hybrid aerogels for methylene blue degradation," *Scientific Reports*, vol. 3, pp. 3018–3026, 2013.

[8] L. Gu, J. Wang, H. Cheng, Y. Zhao, L. Liu, and X. Han, "One-step preparation of graphene-supported anatase TiO_2 with exposed 001 facets and mechanism of enhanced photocatalytic properties," *ACS Applied Materials & Interfaces*, vol. 5, no. 8, pp. 3085–3093, 2013.

[9] J. Yu and J. Ran, "Facile preparation and enhanced photocatalytic H_2-production activity of $Cu(OH)_2$cluster modified TiO_2," *Energy and Environmental Science*, vol. 4, no. 4, pp. 1364–1371, 2011.

[10] H. Bai, Z. Liu, and D. D. Sun, "Facile preparation of monodisperse, carbon doped single crystal rutile TiO_2 nanorod spheres

with a large percentage of reactive (110) facet exposure for highly efficient H_2 generation," *Journal of Materials Chemistry*, vol. 22, no. 36, pp. 18801–18807, 2012.

[11] T. Bak, J. Nowotny, M. Rekas, and C. C. Sorrell, "Photo-electrochemical hydrogen generation from water using solar energy. Materials-related aspects," *International Journal of Hydrogen Energy*, vol. 27, no. 10, pp. 991–1022, 2002.

[12] S. Chuangchote, J. Jitputti, T. Sagawa, and S. Yoshikawa, "Photocatalytic activity for hydrogen evolution of electrospun TiO_2 nanofibers," *ACS Applied Materials and Interfaces*, vol. 1, no. 5, pp. 1140–1143, 2009.

[13] T. Tachikawa, M. Fujitsuka, and T. Majima, "Mechanistic insight into the TiO_2 photocatalytic reactions: design of new photocatalysts," *The Journal of Physical Chemistry C*, vol. 111, no. 14, pp. 5259–5275, 2007.

[14] J. Shi, X. Yan, H. Cui et al., "Low-temperature synthesis of CdS/TiO_2 composite photocatalysts: influence of synthetic procedure on photocatalytic activity under visible light," *Journal of Molecular Catalysis A: Chemical*, vol. 356, pp. 53–60, 2012.

[15] M. Xu, P. Da, H. Wu, D. Zhao, and G. Zheng, "Controlled Sn-doping in TiO_2 nanowire photoanodes with enhanced photoelectrochemical conversion," *Nano Letters*, vol. 12, no. 3, pp. 1503–1508, 2012.

[16] X. Chen, H. Li, T. Sun, and X. Cui, "One step flame assisted pyrolysis synthesis of Fe doped carbon incorporated TiO2 and its photocatalytic activity," *Chemical Journal of Chinese Universities*, vol. 34, no. 12, pp. 2855–2960, 2013.

[17] M. C. Wu, J. Hiltunen, A. Sápi et al., "Nitrogen-doped anatase nanofibers decorated with noble metal nanoparticles for photocatalytic production of hydrogen," *ACS Nano*, vol. 5, no. 6, pp. 5025–5030, 2011.

[18] L. Zhu, J. Xie, X. Cui, J. Shen, X. Yang, and Z. Zhang, "Photoelectrochemical and optical properties of N-doped TiO_2 thin films prepared by oxidation of sputtered TiN_x films," *Vacuum*, vol. 84, no. 6, pp. 797–802, 2010.

[19] P. Song, X. Zhang, M. Sun, X. Cui, and Y. Lin, "Graphene oxide modified TiO_2 nanotube arrays: enhanced visible light photoelectrochemical properties," *Nanoscale*, vol. 4, no. 5, pp. 1800–1804, 2012.

[20] Y. Luo, X. Cui, and J. Xie, "Preparation and visible light photoelectrochemical response of TiO_2 -MoO_3 composite nanotube thin films," *Acta Physico—Chimica Sinica*, vol. 27, no. 1, pp. 135–142, 2011.

[21] H. Wang, T. T. You, W. W. Shi, J. Li, and L. Guo, "Au/TiO_2/Au as a plasmonic coupling photocatalyst," *Journal of Physical Chemistry C*, vol. 116, no. 10, pp. 6490–6494, 2012.

[22] Q. Wang, X. Yang, D. Liu, and J. Zhao, "Fabrication, characterization and photocatalytic properties of Ag nanoparticles modified TiO_2 NTs," *Journal of Alloys and Compounds*, vol. 527, pp. 106–111, 2012.

[23] T. Sreethawong, C. Junbua, and S. Chavadej, "Photocatalytic H_2 production from water splitting under visible light irradiation using Eosin Y-sensitized mesoporous-assembled Pt/TiO_2 nanocrystal photocatalyst," *Journal of Power Sources*, vol. 190, no. 2, pp. 513–524, 2009.

[24] Y. Li, C. Xie, S. Peng, G. Lu, and S. Li, "Eosin Y-sensitized nitrogen-doped TiO_2 for efficient visible light photocatalytic hydrogen evolution," *Journal of Molecular Catalysis A: Chemical*, vol. 282, no. 1-2, pp. 117–123, 2008.

[25] C. Chen, M. Long, H. Zeng et al., "Preparation, characterization and visible-light activity of carbon modified TiO_2 with two kinds of carbonaceous species," *Journal of Molecular Catalysis A: Chemical*, vol. 314, no. 1-2, pp. 35–41, 2009.

[26] J. Zhong, F. Chen, and J. Zhang, "Carbon-deposited TiO_2: synthesis, characterization, and visible photocatalytic performance," *The Journal of Physical Chemistry C*, vol. 114, no. 2, pp. 933–939, 2010.

[27] H. Li, X. Zhang, X. Cui, and Y. Lin, "TiO_2 nanotubes/MWCNTs nanocomposite photocatalysts: synthesis, characterization and photocatalytic hydrogen evolution under UV-vis light illumination," *Journal of Nanoscience and Nanotechnology*, vol. 12, no. 3, pp. 1806–1811, 2012.

[28] X. Y. Zhang, H. P. Li, X. L. Cui, and Y. Lin, "Graphene/TiO_2 nanocomposites: synthesis, characterization and application in hydrogen evolution from water photocatalytic splitting," *Journal of Materials Chemistry*, vol. 20, no. 14, pp. 2801–2806, 2010.

[29] C. Lin, J. Chao, C. Liu, J. Chang, and F. Wang, "Effect of calcination temperature on the structure of a Pt/TiO_2 (B) nanofiber and its photocatalytic activity in generating H_2," *Langmuir*, vol. 24, no. 17, pp. 9907–9915, 2008.

[30] S. Kim, S. Hwang, and W. Choi, "Visible light active platinum-ion-doped TiO_2 photocatalyst," *Journal of Physical Chemistry B*, vol. 109, no. 51, pp. 24260–24267, 2005.

[31] J. Yu, L. Qi, and M. Jaroniec, "Hydrogen production by photocatalytic water splitting over Pt/TiO_2 nanosheets with exposed (001) facets," *The Journal of Physical Chemistry C*, vol. 114, no. 30, pp. 13118–13125, 2010.

[32] S. Shanmugam and A. Gedanken, "Synthesis and electrochemical oxygen reduction of platinum nanoparticles supported on mesoporous TiO_2," *The Journal of Physical Chemistry C*, vol. 113, no. 43, pp. 18707–18712, 2009.

[33] C. Wang, L. Yin, L. Zhang, N. Liu, N. Lun, and Y. Qi, "Platinum-nanoparticle-modified TiO_2 nanowires with enhanced photocatalytic property," *ACS Applied Materials & Interfaces*, vol. 2, no. 11, pp. 3373–3377, 2010.

[34] T. Sreethawong, S. Laehsalee, and S. Chavadej, "Use of Pt/N-doped mesoporous-assembled nanocrystalline TiO_2 for photocatalytic H_2 production under visible light irradiation," *Catalysis Communications*, vol. 10, no. 5, pp. 538–543, 2009.

[35] A. A. Ismail, D. W. Bahnemann, and S. A. Al-Sayari, "Synthesis and photocatalytic properties of nanocrystalline Au, Pd and Pt photodeposited onto mesoporous RuO_2-TiO_2 nanocomposites," *Applied Catalysis A: General*, vol. 431-432, no. 26, pp. 62–68, 2012.

[36] Y. Wang, M. Jing, M. Zhang, and J. Yang, "Facile synthesis and photocatalytic activity of platinum decorated $TiO_{2-x}N_x$: perspective to oxygen vacancies and chemical state of dopants," *Catalysis Communications*, vol. 20, pp. 46–50, 2012.

[37] X. Zhang, Y. Sun, X. Cui, and Z. Jiang, "Carbon-incorporated TiO_2 microspheres: facile flame assisted hydrolysis of tetrabutyl orthotitanate and photocatalytic hydrogen production," *International Journal of Hydrogen Energy*, vol. 37, no. 2, pp. 1356–1365, 2012.

[38] H. Li, X. Ma, and X. Cui, "Facile flame thermal synthesis of SiO_x-C/ TiO_2 microspheres with enhanced photocatalytic performance," *Materials Research Express*, vol. 1, Article ID 025502, 2014.

[39] W. Li, J. Yang, Z. Wu et al., "A versatile kinetics-controlled coating method to construct uniform porous TiO_2 shells for multifunctional core-shell structures," *Journal of the American Chemical Society*, vol. 134, no. 29, pp. 11864–11867, 2012.

[40] H. Ma and H. Yang, "A comparative study of TiO_2 nanoparticles synthesized in premixed and diffusion flames," *Journal of Thermal Science*, vol. 19, no. 6, pp. 567–575, 2010.

[41] M. Giannouri, Th. Kalampaliki, N. Todorova et al., "One-Step synthesis of TiO_2/perlite composites by flame spray pyrolysis and their photocatalytic behavior," *International Journal of Photoenergy*, vol. 2013, Article ID 729460, 8 pages, 2013.

[42] D. L. Swihart and W. R. Mason, "Electronic spectra of octahedral platinum(IV) complexes," *Inorganic Chemistry*, vol. 9, no. 7, pp. 1749–1757, 1970.

[43] H. Einaga and M. Harada, "Photochemical preparation of poly(N-vinyl-2-pyrrolidone)-stabilized platinum colloids and their deposition on titanium dioxide," *Langmuir*, vol. 21, no. 6, pp. 2578–2584, 2005.

[44] M. A. Ahmed, "Synthesis and structural features of mesoporous NiO/TiO_2 nanocomposites prepared by sol-gel method for photodegradation of methylene blue dye," *Journal of Photochemistry and Photobiology A: Chemistry*, vol. 238, pp. 63–70, 2012.

[45] C. Lettmann, K. Hildenbrand, H. Kisch, W. Macyk, and W. F. Maier, "Visible light photodegradation of 4-chlorophenol with a coke-containing titanium dioxide photocatalyst," *Applied Catalysis B: Environmental*, vol. 32, no. 4, pp. 215–227, 2001.

[46] X. Li, Z. Zhuang, W. Li, and H. Pan, "Photocatalytic reduction of CO_2 over noble metal-loaded and nitrogen-doped mesoporous TiO_2," *Applied Catalysis A: General*, vol. 429-430, pp. 31–38, 2012.

[47] O. C. Comptons, C. H. Mullet, S. Chiang, and F. E. Osterloh, "A building block approach to photochemical water-splitting catalysts based on layered niobate nanosheets," *The Journal of Physical Chemistry C*, vol. 112, no. 15, pp. 6202–6208, 2008.

[48] Z. Zheng, B. Huang, X. Qin, X. Zhang, Y. Dai, and M. Whangbo, "Facile in situ synthesis of visible-light plasmonic photocatalysts $M@TiO_2$ (M = Au, Pt, Ag) and evaluation of their photocatalytic oxidation of benzene to phenol," *Journal of Materials Chemistry*, vol. 21, no. 25, pp. 9079–9087, 2011.

[49] R. Wang, N. Sakai, A. Fujishima, T. Watanabe, and K. Hashimoto, "Studies of surface wettability conversion on TiO_2 single-crystal surfaces," *Journal of Physical Chemistry B*, vol. 103, no. 12, pp. 2188–2194, 1999.

[50] A. O. T. Patrocínio, E. B. Paniago, R. M. Paniago, and N. Y. M. Iha, "XPS characterization of sensitized n-TiO_2 thin films for dye-sensitized solar cell applications," *Applied Surface Science*, vol. 254, no. 6, pp. 1874–1879, 2008.

[51] W. Ren, Z. Ai, F. Jia, L. Zhang, X. Fan, and Z. Zou, "Low temperature preparation and visible light photocatalytic activity of mesoporous carbon-doped crystalline TiO_2," *Applied Catalysis B: Environmental*, vol. 69, no. 3-4, pp. 138–144, 2007.

[52] J. A. Rengifo-Herrera, K. Pierzchała, A. Sienkiewicz et al., "Synthesis, characterization, and photocatalytic activities of nanoparticulate N, S-codoped TiO_2 having different surface-to-volume ratios," *The Journal of Physical Chemistry C*, vol. 114, no. 6, pp. 2717–2723, 2010.

[53] L. P. Xiong, S. Hu, J. W. Hou, K. P. Weng, Y. M. Luo, and T. Z. Yang, "Preparation and catalytic activity of Pt based hydrophobic catalysts adulterated with Fe series elements," *Journal of Inorganic Materials*, vol. 26, no. 1, pp. 91–96, 2011.

[54] H. Xu, X. Chen, S. Ouyang, T. Kako, and J. Ye, "Size-dependent Mie's scattering effect on TiO_2 spheres for the superior photoactivity of H_2 evolution," *The Journal of Physical Chemistry C*, vol. 116, no. 5, pp. 3833–3839, 2012.

[55] P. Cheng, Z. Yang, H. Wang et al., "TiO_2-graphene nanocomposites for photocatalytic hydrogen production from splitting water," *International Journal of Hydrogen Energy*, vol. 37, no. 3, pp. 2224–2230, 2012.

[56] X. Zhang, Y. Sun, X. Cui, and Z. Jiang, "A green and facile synthesis of TiO_2/graphene nanocomposites and their photocatalytic activity for hydrogen evolution," *International Journal of Hydrogen Energy*, vol. 37, no. 1, pp. 811–815, 2012.

[57] W. Lin, W. Yang, I. Huang, T. Wu, and Z. Chung, "Hydrogen production from methanol/water photocatalytic decomposition using $Pt/TiO_{2-x}N_x$ catalyst," *Energy & Fuels*, vol. 23, no. 4, pp. 2192–2196, 2009.

[58] M. Zhu, Z. Li, B. Xiao et al., "Surfactant assistance in improvement of photocatalytic hydrogen production with the porphyrin noncovalently functionalized graphene nanocomposite," *ACS Applied Materials and Interfaces*, vol. 5, no. 5, pp. 1732–1740, 2013.

[59] C. C. Lin, T. Y. Wei, K. T. Lee, and S. Y. Lu, "Titania and Pt/titania aerogels as superior mesoporous structures for photocatalytic water splitting," *Journal of Materials Chemistry*, vol. 21, no. 34, pp. 12668–12674, 2011.

[60] P. Wei, J. Liu, and Z. Li, "Effect of Pt loading and calcination temperature on the photocatalytic hydrogen production activity of TiO_2 microspheres," *Ceramics International*, vol. 39, no. 5, pp. 5387–5391, 2013.